Journal of Electroanalytical Chemistry 701 (2013) 50–58

Contents lists available at SciVerse ScienceDirect

Journal of Electroanalytical Chemistry

journal homepage: www.elsevier.com/locate/jelechem

Tailoring the current density to enhance photocatalytic activity of CuO/HY for decolorization of malachite green

A.A. Jalil [a,*], M.A.H. Satar [a], S. Triwahyono [b], H.D. Setiabudi [a], N.H.N. Kamarudin [a], N.F. Jaafar [b], N. Sapawe [a], R. Ahamad [c]

[a] Institute of Hydrogen Economy, Department of Chemical Engineering, Faculty of Chemical Engineering, Universiti Teknologi Malaysia, 81310 UTM Johor Bahru, Johor, Malaysia
[b] Ibnu Sina Institute for Fundamental Science Studies, Faculty of Science, Universiti Teknologi Malaysia, 81310 UTM Johor Bahru, Johor, Malaysia
[c] Department of Chemistry, Faculty of Science, Universiti Teknologi Malaysia, 81310 UTM Johor Bahru, Johor, Malaysia

ARTICLE INFO

Article history:
Received 8 December 2012
Received in revised form 13 April 2013
Accepted 6 May 2013
Available online 16 May 2013

Keywords:
Isomorphous substitution
CuO/HY catalyst
Current density
Malachite green
Photodecolorization

ABSTRACT

CuO supported on HY zeolite (CuO/HY) catalyst was prepared via a simple electrolysis method under different levels of current density, and its properties and photoactive performance were investigated. The physicochemical properties of the catalyst were examined using X-ray Diffraction (XRD), surface area analysis, Ultraviolet–Visible Diffuse Reflectance Spectroscopy (UV–Vis DRS), Fourier Transform Infrared (FTIR) spectroscopy, and pyridine adsorption FTIR. The analyses indicated that CuO/HY catalyst contains both CuO nanoparticles and incorporation of copper into the HY framework. In parallel with the formation of Cu^0 in the electrolysis system, the Cu^{2+} ions also underwent isomorphous substitution subsequent to dealumination to form a Si–Cu–O bond, as confirmed by the FTIR result. The formation of the Si–Cu–O bond was found to decrease at elevated current density and this lowered the photocatalytic decolorization of malachite green (MG) by CuO/HY. The CuO/HY prepared at 10 mA cm^{-2} was the optimum catalyst and produced complete and 50% decolorization of 10 and 15 mg L^{-1} of MG, respectively. The results indicating the decrease in chemical oxygen demand (COD) and total organic carbon (TOC) demonstrated the degradability of MG molecules. The CuO/HY is also stable and showed no leaching effect even after six reaction cycles, with just small decreases in the decolorization percentage (<89%). The catalyst has the potential to be applied in textile wastewater treatment which is always in low concentration level. It is also believed that this study will be useful for synthesis of other catalysts that necessitate a degree of isomorphous substitution of metal ions in a zeolite network.

1. Introduction

Up to 200,000 tons/year of dyes, used extensively in various textile industries, are discharged into the effluent during drying and finishing operations [1]. This is an important source of environmental pollution. Therefore, treatment of the wastewater is necessary before releasing it into the environment because the dyes are carcinogenic and mutagenic and inhibit photosynthesis. Three main treatment techniques have been applied for the removal of dyes from wastewater including physical, chemical, and biological methods. However, biological and physical processes are always reported as ineffective methods [2] and generate secondary waste [3]. Therefore, the use of a heterogeneous photocatalyst for wastewater treatment has become more popular because it can be operated in mild conditions and transforms the toxic organic pollutants into nontoxic products [4,5].

Recently, copper oxide (CuO) photocatalyst has received much attention from researchers due to its narrow band gap (≈1.7 eV), low cost, low toxicity, and high availability [6,7]. It has been also reported to be more photoreactive than Al_2O_3, ZnO, and NiO [6]. Accordingly, many techniques have been developed for the synthesis of nanosized CuO, including microwave radiation, impregnation, co-precipitation, and the sol–gel method [8–10]. However, the size control, size distribution, shape, degree of acidity, and so on, remains a challenge [11]. Later, it has been reported that CuO on various supporting matrixes such as zeolites and mesoporous materials could enhance the photoactivity of the catalysts [7,12]. The high surface area and cation exchange capabilities of such materials offer good interactions with the metal oxides and improve the properties of the catalysts [13].

We have reported a new method for the preparation of zinc metal nanoparticles by a simple electrochemical technique and its successful use in the synthesis of various types of drug precursors [14,15]. By applying the corresponding method, Zn and Ni promoted on zeolite catalysts led to efficient isomerization of petrochemical products [16–18]. Recently, we also reported the

* Corresponding author. Tel.: +60 7 5535581; fax: +60 7 5536165.
E-mail address: aishah@cheme.utm.my (A.A. Jalil).

1572-6657/$ - see front matter © 2013 Elsevier B.V. All rights reserved.
http://dx.doi.org/10.1016/j.jelechem.2013.05.003

preparation of highly photoreactive α-Fe_2O_3, ZrO_2 and ZnO supported on HY zeolite catalysts for efficient decolorization of dyes [19–21]. Although the metal/metal supported catalysts were prepared by the same technique, they underwent different synthesis mechanisms, which led to different properties in terms of particle size, acidity, and structure, which gave advantages to their application.

It was also found that variation of the electrolysis conditions such as temperature, current density, type of solvents, and so on affects the efficiency of the subsequent applied organic reactions [22,23]. However, until now there is no detailed report relating the effect of such specific electrolysis conditions on the physicochemical properties of the supported metal oxide catalysts. New findings regarding this matter would be advantageous for the design of new catalysts for various applications because the corresponding electrosynthesis method is very facile as the catalyst can be prepared in a short time without using metal salts solutions. Recently, we found that the properties and photoactive performance of the metal supported on zeolite catalysts were strongly affected by the current density applied during electrolysis. Therefore, in this study we report, for the first time, on the effect of the level of current density on the physicochemical properties of CuO supported on HY zeolite (CuO/HY) catalyst. The characterization of the catalyst was carried out by X-ray Diffraction (XRD), surface area analysis, Ultraviolet–Visible Diffuse Reflectance Spectroscopy (UV–Vis DRS), Fourier Transform Infrared (FTIR) spectroscopy, and pyridine adsorption FTIR. The performance of CuO/HY prepared under different levels of current density for the photodecolorization of malachite green (MG) dye under fluorescent lamp irradiation was examined. Different levels of current density were found to affect the dealumination of the HY framework, ion exchange capacity, particle size, and acidity of the catalysts, which then influenced the band gap and subsequent MG photodecolorization. The activation energy, kinetics, and reusability of the catalysts were also investigated in detail.

2. Materials and methods

2.1. Materials

HY zeolite (Zeolyst International, USA, Si/Al = 80) was used as a support for CuO. Naphthalene (Fluka Chemie) was used as a mediator in the electrolysis reaction. Platinum and copper plate cells (Nilaco and Tanaka Metal Corporation, Japan) were utilized as electrodes. Hydrochloric acid and sodium hydroxide were added to adjust the pH of the sample solution. *N*,*N*-dimethylformamide (DMF) was used as solvent, and MG was used as an organic pollutant. All reagents were purchased from Merck (USA).

2.2. Preparation of the catalyst

The CuO loading on the HY support was maintained at 5 wt% for all catalysts studied. The procedure for the preparation of 5 wt% CuO/HY catalyst was as follows: a DMF solution was added to a one-compartment cell fitted with a platinum plate cathode (2 cm × 2 cm) and a copper plate anode (2 cm × 2 cm) containing tetraethylammonium perchlorate, naphthalene, and HY zeolite. Naphthalene was added as a mediator to accelerate the reaction by producing anion radicals for the reduction of the copper cations [22]. Then, the electrolysis was conducted at a constant current of 10 mA cm^{-2} and 273 K under an N_2 atmosphere. The required copper loading on the HY support was calculated based on Faraday's law of electrolysis. After electrolysis, the mixture was impregnated at 353 K in an oil bath before being dried overnight at 373 K and calcined for 3 h at 823 K to give gray-colored CuO/HY. The 5 wt% CuO/HY was prepared under three different levels of current density by adjusting the electrolysis time according to the Faraday's law of electrolysis, which were 10, 30 and 120 mA cm^{-2} in 99.9, 33.3 and 8.32 min, respectively.

2.3. Characterization of the catalysts

The properties of catalysts were determined using differential analytical techniques. XRD patterns of the catalysts were obtained using a Bruker Advance D8 X-ray powder diffractometer with a Cu Kα (λ = 1.5418 Å) radiation source. The UV–Vis diffuse reflectance spectroscopic studies were carried out using a Perkin Elmer Lambda 900 UV/VIS/NIR spectrometer with an integrating sphere. The surface area was calculated with the Brunauer–Emmett–Teller (BET) method, and pore distributions were determined by the Barrett–Joyner–Halender (BJH) method whereas the micropore area, micropore volume, and external surface area were estimated by t-plots. FTIR spectra were obtained with a KBr pellet using a Perkin Elmer GX FTIR spectrometer over the range of 4000–370 cm^{-1}.

2.4. Photocatalytic activity measurement

The photocatalytic testing was carried out by placing a dosage of 0.38 g L^{-1} of catalyst in a 200 mL MG solution at a certain concentration and stirring in the dark for 2 h in a batch reactor to allow the mixture to reach the adsorption–desorption equilibrium. A fluorescent lamp with a definite power of 20 W as the light source was mounted above 10 cm of the solution. The entire system was placed inside a chamber covered with aluminum foil to prevent the passage of other light into the reactor. During irradiation, aliquots of approximately 2 ml of the solution were taken at intervals of 30 min over a 3 h period. The concentration of the samples was verified by measuring their absorption band at 616 nm, the λ_{max} of MG, using a UV–Vis spectrophotometer. The decolorization efficiency was calculated as follows:

$$\text{Decolorization}\% = \left(\frac{A_i - A_t}{A_i}\right) \times 100 \quad (1)$$

where A_i is initial absorbance of the MG and A_t is absorbance of the MG at any time interval after irradiation of the MG at 616 nm.

The COD test values were measured using a HACH DR4000 spectrometer and COD reactor. A Shimadzu TOC-VCPH spectrophotometer was used for TOC measurements in each experiment before and after a reaction time of 180 min for evaluation of the mineralization of MG dye.

3. Result and discussion

3.1. Characterization of the catalyst

3.1.1. XRD

Fig. 1 illustrates the XRD pattern of HY zeolite and 5 wt% CuO/HY catalysts which were prepared under three different current densities: 10, 30, and 120 mA cm^{-2}. No other diffraction peaks were observed except HY, indicating the absence of any structural damage to the catalysts [24]. The peak intensity of HY decreased as the current density increased, most probably due to the presence of copper oxide, which affects the morphology of the HY fingerprint. In fact, our previous study confirmed that the diffraction peaks at 2θ = 35.15° and 38.45°, which are shown in the inset, correspond to the peaks of copper oxide. Similar results showing that the peaks between 2θ = 35° and 39° correspond to the formation of copper oxide have also been reported in the literature [8,10].

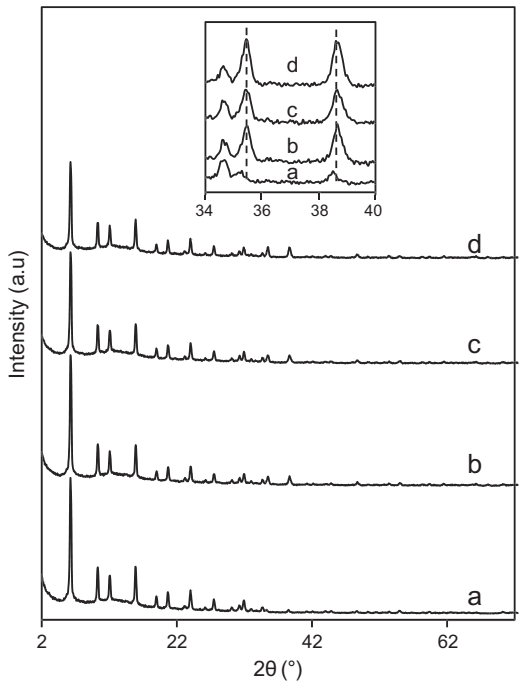

Fig. 1. XRD patterns of (a) HY and 5 wt% CuO/HY catalysts prepared under current density of, (b) 10 mA cm^{-2}, (c) 30 mA cm^{-2} and (d) 120 mA cm^{-2}.

The prominent peak was used to roughly estimate the average crystallite size of CuO in the CuO/HY by using the Debye–Scherrer equation:

$$D = \frac{k\lambda}{\beta \cos\theta} \tag{2}$$

where k = 0.94 is a coefficient, λ = 1.541 Å is the X-ray wavelength, β is the full width at half maximum (FWHM) of the peak, and θ is the diffraction angle at 38.5°. As tabulated in Table 1, the increase in current density was found to decrease the particle size of the catalyst.

3.1.2. Specific surface area analysis

The specific surface area and pore volume of pure HY and 5 wt% CuO/HY catalysts prepared under different current densities are presented in Table 1. The results showed that the CuO loading onto HY support decreased the specific surface area and pore volume of the catalyst. This is most probably due to the presence of CuO and the incorporation of CuO in the HY framework [19,20]. The restructuring of the catalyst may occurs when the larger size of Cu^{2+} ion was exchanged with the Al^{3+} ion in the HY framework. A similar result showing that the pore volume decreased with incorporation of the CuO in zeolite framework was also reported in the literature [6].

The increase in current density was found to increase the specific surface area and pore volume of the catalyst. This result is in agreement with the result for the crystallite size of the catalyst calculated by the Scherrer equation (Section 3.1.1), in which a rise in the current density caused the particle size to decrease (Table 1). It was also reported that the elevated current density in a similar system enhanced the reactivity of zinc metal towards production of organozinc compounds, implying a higher specific surface area and smaller particle size of zinc metals prepared under a higher current density compared to a lower current density [23]. The result of BJH analysis shown in Fig. 2 indicates that the CuO/HY prepared under higher current density produced more pore blockage than that prepared under lower current density, illustrating the smaller particle sizes of catalyst prepared at 120 mA cm^{-2} in comparison to preparation at 30 and 10 mA cm^{-2}.

3.1.3. UV–Vis DRS and band gap determination

The UV–Vis DRS profile of HY, pure electrolyzed CuO, and CuO/HY catalysts prepared under different current densities are shown in Fig. 3. The pure CuO shows a very strong adsorption band at 260 nm and a broad band in the range of 380–780 nm [25]. For CuO/HY, the spectroscopy appears to be significantly affected by the introduction of CuO. All catalysts showed a weak broad band in the range of 380–750 nm which not observable in pure HY, confirming the adsorption band for copper oxide species [26,27]. In addition, there are no adsorption bands around 340–360 nm, assigning the absence of Cu clusters on the support, which indicated that the CuO nanoparticles were in a highly dispersed state [26].

Band gap energy is an important factor for catalysts in photocatalytic reactions. An accurate value of the band gap energy can be obtained by recording the spectra in reflection mode rather than absorption spectra in order to minimize the scattering effect [28]. The band gap energy was determined by using the following equation [29],

$$K = \frac{(1-R)^2}{2R} = F(R) \tag{3}$$

where K is the reflectance transformed according to Kubelka Munk and R is the reflectancy (%) from the sample by plotting the function $(K*hv)^{1/2}$ versus hv and extrapolating the linear part of the curve to $(K*hv)^{1/2} = 0$, as demonstrated in Fig. 4. It was found that the values of band gap energy for CuO/HY catalysts prepared at 10, 30, and 120 mA cm^{-2} were 1.20, 1.40, and 1.70 eV, respectively; in other words they increased with increasing current density. This may be attributed to the quantum size effect (QSE), as supported by the XRD and surface area analysis results, which indicate that the increase in current density led to the decrease in the particle size [30]. The QSE led to discretization of energy bands and resulted in widening of the band gap [31].

3.1.4. FTIR

The FTIR spectra of pure HY and CuO/HY prepared under varying current densities are shown in Fig. 5. The CuO/HY catalysts showed bands of varying intensity and width that were typical for pure HY at about 1177, 1079, 790, 530, and 460 cm^{-1}, which corresponded to internal and external vibration of $(Si,Al)O_4$ of the HY framework (Fig. 5A) [32,33]. The spectra of CuO/HY catalysts'

Table 1
Specific surface area of HY and CuO/HY catalysts with varying current densities.

Catalyst	Crystal size (nm)[a]	Surface area ($m^2\ g^{-1}$)	Pore volume ($cm^3\ g^{-1}$)
HY	23.2	654	0.445
CuO/HY (10 mA cm^{-2})	23.0	576	0.424
CuO/HY (30 mA cm^{-2})	21.2	579	0.426
CuO/HY (120 mA cm^{-2})	20.5	585	0.431

[a] Determined by XRD using Debye–Scherrer equation.

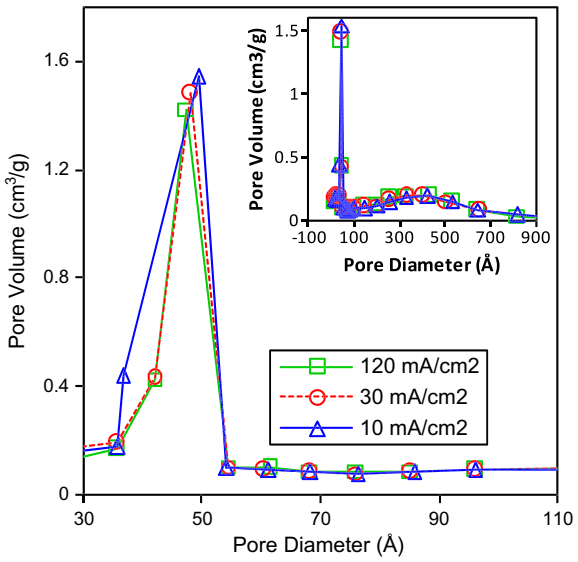

Fig. 2. Pore size distribution curves of CuO/HY prepared under 10, 30 and 120 mA cm^{-2}.

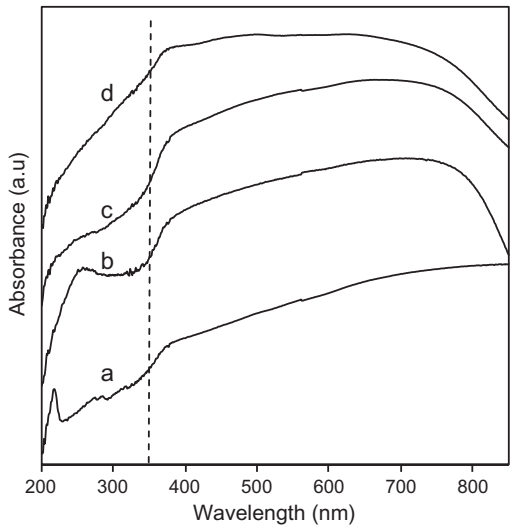

Fig. 3. UV–Vis reflectance spectra of the (a) pure HY, (b) CuO, (c) CuO/HY prepared at 10 mA cm^{-2}, (d) CuO/HY 30 mA cm^{-2} and (e) CuO/HY 120 mA cm^{-2}.

bands did not show significant changes compared with pure HY. However, a sharp band at 613 cm^{-1} which corresponds to an Si–O–M bond (M refers to either Al or Cu) was found to increase with copper loading (Fig. 5Ba) but decrease with increasing current density (Fig. 5Bb–Bd), indicating the possible interaction of copper in the HY structure instead of Si–O–Al (Fig. 5B) [34,35]. This may be due to an isomorphous substitution of Cu that occurred in the framework of aluminosilicate HY after the dealumination [20]. A new peak appeared clearly in the 575 cm^{-1} band when the catalyst was prepared under a current density of 120 mA cm^{-2}, which may correspond to a vibration of Cu(II)–O [36]. This result is well matched with the XRD data, indicating the presence of copper oxide particles in the HY. According to these results, it could be stated that the lower the current density the longer the electrolysis time (Table 1), which allowed more dealumination to occur in the system, accompanied by isomorphous substitution, resulting in more formation of Si–O–Cu bonds in the HY framework [20]. However, due to the limited electrolysis time, exactly the same

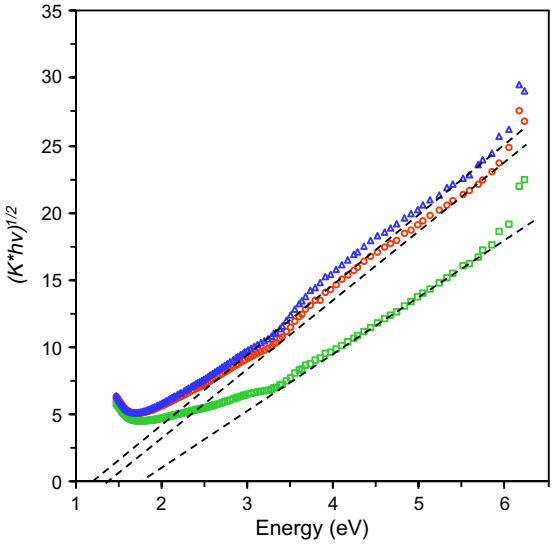

Fig. 4. The band gap energy calculation by Kubelka–Munk plot for prepared CuO/HY catalysts varying current density. (△) 10 mA cm^{-2} (○) 30 mA cm^{-2} (□) 120 mA cm^{-2}.

phenomenon did not take place in the system at higher current density (120 mA cm^{-1}), the unbounded copper oxide species was more dominant compared to incorporated CuO, and it is presumed that the CuO nanoparticles were distributed well on the HY surface, as verified by the results shown in Figs. 1 and 5Bd [20]. The greater pore blockage demonstrated by the CuO/HY prepared at higher current density could also support this result (Fig. 2).

To clarify this hypothesis, the evacuated FTIR analysis was performed at 673 K for 1 h in order to further study the hydroxyl group involved in the catalysts' structure. As shown in Fig. 5C, the spectrum of pure HY gave two bands at 3745 and 3740 cm^{-1} and a small absorption band at 3700 cm^{-1} due to the germinal, terminal silanol group and a hydroxyl group in a defect site of the HY framework, respectively [37]. The peak at 3745 cm^{-1} disappeared with elevated current density, suggesting that a weak interaction occurred between the isolated silanol groups and the neighboring metal species [38]. Krijnen also reported that the shift of the peak from 3745 to 3740 cm^{-1} may be due to the dealumination that occurs in the zeolite. The peak at 3700 cm^{-1} decreased in intensity as the copper was loaded onto HY, which is a sign of the interaction of Cu species with weak hydrogen bridges in defect sites of hydroxyl groups. A new peak was observed at 3660 cm^{-1}, which increased in intensity with decreasing current density, indicating that the amount of hydroxyl groups of the extra framework aluminum species (Al(O)OH) increased when the current density decreased. These results support the above observation that more dealumination occurred when the current density was lower, leading to more isomorphous substitution of Cu in the framework of aluminosilicate HY [19,20].

3.1.5. Pyridine adsorption FTIR

Fig. 6 shows the infrared spectra of pyridine adsorbed onto HY and 5 wt% CuO/HY catalysts prepared under 10, 30, and 120 mA cm^{-2} of current density. The spectra exhibit both the expected bands assignable to pyridine bound on Brønsted acid sites (1545–1550 cm^{-1}) and pyridine bound on Lewis acid sites (1430–1460 cm^{-1}). Generally, Brønsted sites are attributed to the bridging hydroxyls neighboring the tetrahedrally coordinated Al sites, and Lewis acid sites can be assigned to aluminum in defect positions or to extra framework Al species [39]. It can be observed from Fig. 6 that the peak of Lewis acid sites of HY shifted to a higher wavenumber when the copper was added, indicating the

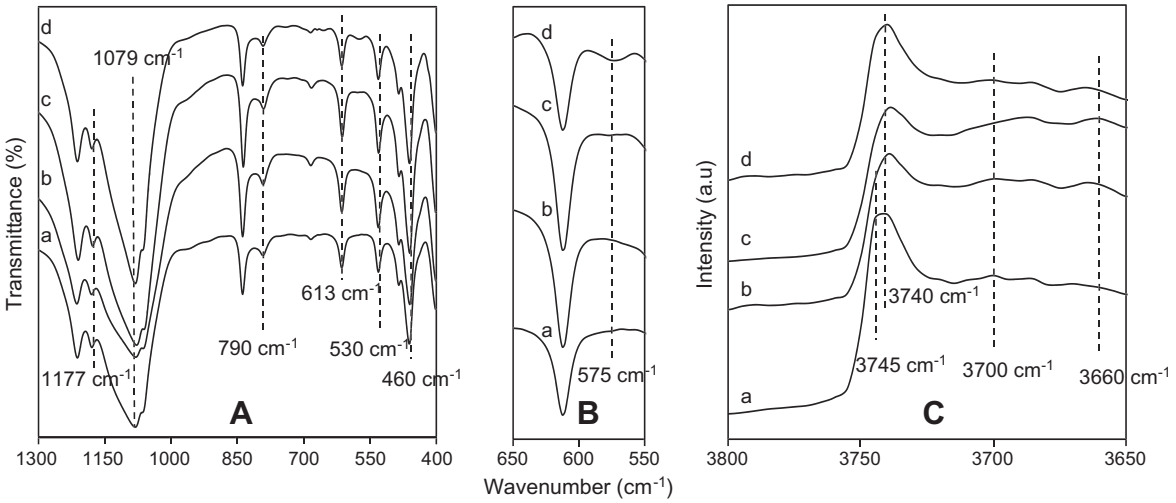

Fig. 5. FTIR patterns of (a) HY and the prepared 5 wt% CuO/HY catalysts with varying current density, (b) 10, (c) 30 and (d) 120 mA cm^{-2}.

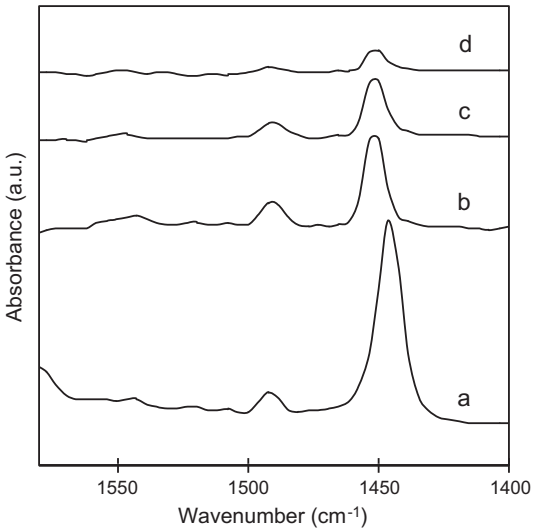

Fig. 6. FTIR spectra of adsorbed pyridine on (a) HY and the prepared 5 wt% CuO/HY catalysts with varying current density, (b) 10, (c) 30 and (d) 120 mA cm^{-2}.

exchange of copper ions with Al in the HY framework [16]. The number of Brønsted sites was not very different from the parent peak but the number of Lewis sites decreased significantly when the current density increased. This result indicates that less dealumination and isomorphous substitution of Cu ions occurred at elevated current density.

3.1.6. Proposed mechanism

In accordance with the above results, the probable reaction mechanism in the preparation of CuO/HY catalyst under different current densities is demonstrated in Fig. 7. Similar to our previous study, electrolysis of a DMF solution results in anodic dissolution of Cu metal at a Cu anode, with the Cu cation being reduced at a Pt cathode via transfer of electrons from the naphthalene radical anion to give zero-valent Cu metal nanoparticles [20,22]. Naphthalene reacts as a mediator in the system and is preferentially reduced prior to the Cu cation, which could be observed instantly as a dark green color cloud-like on the surface of the cathode after the current was started. The cyclic voltammetry was also carried out to verify this occurrence and the result is shown in inset figure. The voltammogram was done in 0.1 M TEAP–DMF using an Ag/Ag^{+} reference electrode. It was observed that the naphthalene was reduced prior to Cu^{2+} in the DMF solution. This result was also in line with the previous study, which showed that naphthalene was reduced prior to Zn^{2+} in the same DMF system [23]. In parallel, the copper cation was also exchanged with the aluminum ion in the aluminosilicate framework of HY via isomorphous substitution to give incorporated CuO, which was proved by the FTIR results. In fact, the dealumination and isomorphous substitution occurred during electrolysis, but not during calcination, as confirmed by our previous study [19]. The pure Cu metal was oxidized to CuO under calcination and presumably distributed well on the surface of the HY support, as confirmed by the XRD, UV–Vis, FTIR, and surface area analyses. The lower the current density applied to the system, the longer the electrolysis time required to produce the same mass of Cu loading, and thus seemingly higher numbers of Cu cations are substituted with the Al in the HY framework. However, a higher current density tends to produce CuO nanoparticles which are smaller in size, as reported by Kurono et al. [23].

3.2. Photocatalytic activity

3.2.1. Performance of the catalysts

The performance of the catalysts prepared under different current densities for the decolorization of MG under fluorescent lamp irradiation was tested, and the results are shown in Fig. 8. All of the catalysts present high photocatalytic activity which completely decolorizes 10 mg L^{-1} of MG after 180 min of reaction. Another series of experiments performed on 15 mg L^{-1} of initial MG concentration led to only 50, 41, and 26% decolorization when using CuO/HY prepared at current densities of 10, 30, and 120 mA cm^{-2}, respectively. These results demonstrate the compatibility of the CuO/HY catalyst for application in wastewater treatment of textile industry effluents, which are always at low concentration [40].

The results indicate that the CuO/HY catalysts prepared at 10 mA cm^{-2} have higher photoactivity compared to those prepared at 30 and 120 mA cm^{-2}, which may be attributed to the narrower band gap of this catalyst, which facilitates excitation of electrons from the valence band to the conduction band, leading to the production of hydroxyl radicals [41]. It appears that the incorporated CuO plays an important role in the photocatalytic reaction rather than the unbounded CuO species. In fact, the Cu^{2+} of the incorporated CuO are active catalytic species that led to the formation of three highly reactive radicals including the $^{\cdot}OH$, $HO_2^{\cdot}$ and $O_2^{\cdot-}$

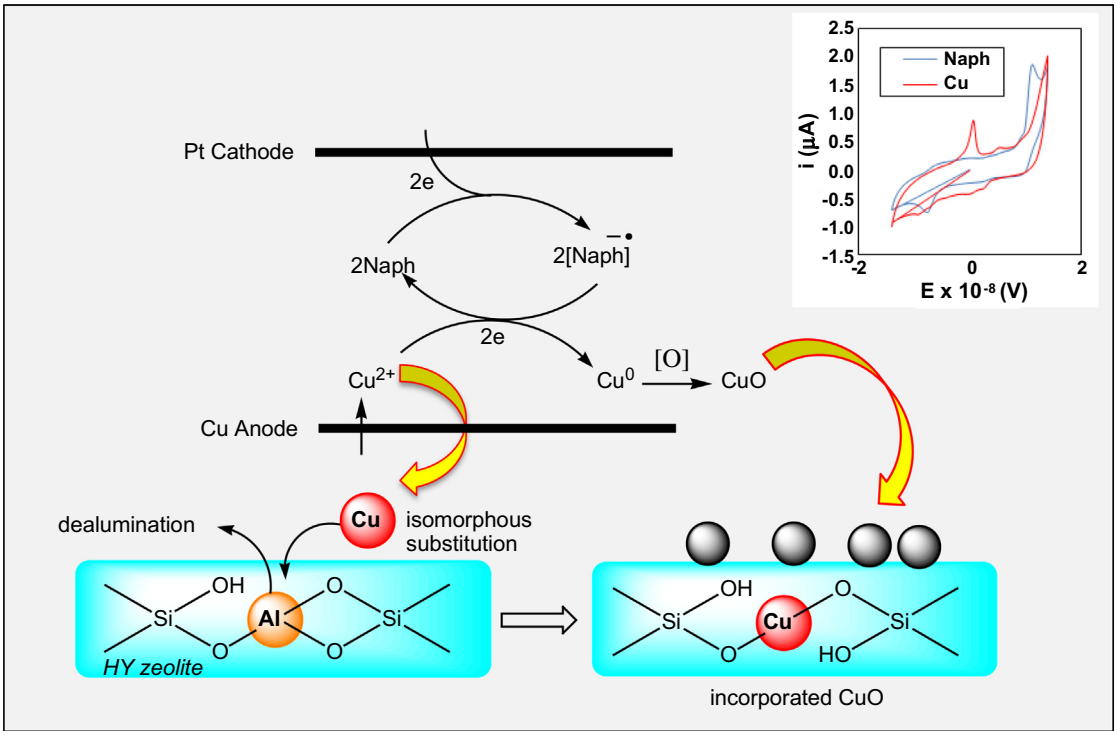

Fig. 7. Proposed reaction mechanism of preparation of CuO/HY and cyclic voltammetry (as inset).

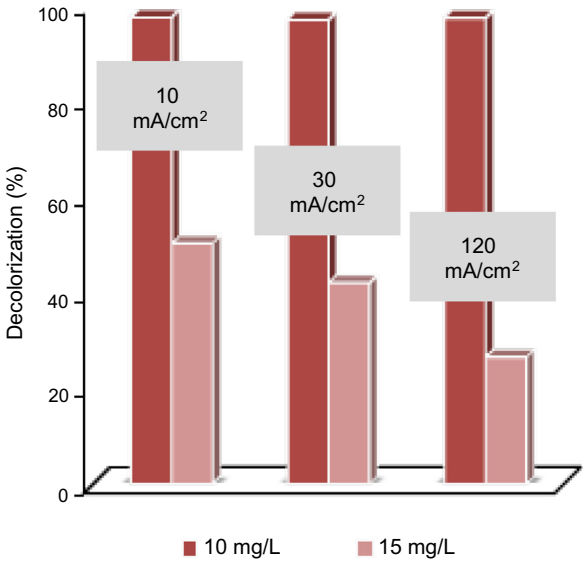

Fig. 8. Performance of the prepared catalysts on decolorization of MG (pH 4, 0.38 g L^{-1}, 10 and 15 mg L^{-1} initial MG concentration).

radicals that participated in the MG photocatalytic decolorization. The irradiation of CuO/HY generated an electron–hole pair and Cu^{2+} ions [35],

$$CuO + h\nu \rightarrow CuO(h^{+}_{VB} + e^{-}_{CB}) \quad (4)$$

$$CuO(Cu^{2+}) \rightarrow CuO_{vacancy} + Cu^{2+} \quad (5)$$

The electron in the conduction band (e^{-}_{CB}) is highly potential and negatively enough to reduce Cu^{2+} to Cu^{+} and then re–oxidize Cu^{+} to Cu^{2+} to ensure the formation of $O^{\cdot}_2$ radicals. Subsequent reaction of the Cu^{+} with the partial $O^{\cdot}_2$ radicals results in the formation of H_2O_2.

$$CuO(Cu^{2+}) + e^{-}_{CB} \rightarrow CuO(Cu^{+}) \quad (6)$$

$$CuO(Cu^{+}) + O_2 \rightarrow CuO(Cu^{2+}) + O^{\cdot}_2 \quad (7)$$

$$H^{+} + O^{\cdot}_2 \rightarrow HO^{\cdot}_2(\textit{partial } O^{\cdot}_2) \quad (8)$$

$$CuO(Cu^{+}) + HO^{\cdot}_2(\textit{partial } O^{\cdot}_2) + H^{+} \rightarrow CuO(Cu^{2+}) + H_2O_2 \quad (9)$$

On the other hand, the valence band hole (h^{+}_{VB}) is positively enough to generate free ·OH and led to direct (Eq. (18)) and indirect (Eqs. (11) and (17)) oxidation of the dye.

$$OH^{-}_{ads} + h^{+}_{VB} \rightarrow {\cdot}OH_{ads} \quad (10)$$

$$H_2O_{ads} + h^{+}_{VB} \rightarrow {\cdot}OH_{ads} + H^{+} \quad (11)$$

The electrons in the conduction band (e^{-}_{CB}) on the catalyst surface can also reduced O_2 to O^{-}_2 (Eq. (12)).

$$O_{2(ads)} + e^{-}_{CB} \rightarrow {\cdot}O^{-}_{2(ads)} \quad (12)$$

The O^{-}_2 species is responsible for the production of free hydroxyl and hydrogen peroxides radicals:

$${\cdot}O^{-}_{2(ads)} + H^{+} \rightarrow HO^{\cdot}_{2(ads)} (\text{in acidic medium}) \quad (13)$$

$$2OH^{\cdot}_{ads} \rightarrow O_2 + H_2O_2 \quad (14)$$

$$H_2O_2 + {\cdot}O^{-}_{2(ads)} \rightarrow O_2 + HO^{\cdot} + HO^{-} \quad (15)$$

$${\cdot}O^{-}_{2(ads)} + HO^{\cdot}_{2(ads)} + H^{+} \rightarrow H_2O_{2+}O_2 \quad (16)$$

Thus, it can be concluded that the Cu^{2+} of the CuO are active catalytic species that led to the formation of three highly reactive radicals including the ·OH, $HO^{\cdot}_2$ and $O^{\cdot}_2$ radicals that participated in the MG oxidation. The high oxidation potential of the holes (h^{+}_{VB}) in the catalyst also permits the direct oxidation of MB to reactive intermediates.

$$\text{Dye} + OH^{\cdot} \rightarrow \text{decolorization of dye} \quad (17)$$

$$\text{Dye} + h^{+}_{VB} \rightarrow \text{oxidation of dye} \quad (18)$$

$$\text{Dye} + e^{-}_{CB} \rightarrow \text{reduction of dye} \quad (19)$$

As a comparison, the photodecolorization was also conducted using a non-electrochemically catalyst, in which the commercial CuO was impregnated with HY zeolite. Only 68% of 10 mg L^{-1} MG was decolorized (figure not shown), this may be due to the lack of active sites of Si–O–Cu bonds which play important role in the photodecolorization [19,20]. In addition, the agglomeration of commercial CuO on the surface of HY might also lead to the lower decolorization. In contrast, electrolysis allowed the dealumination accompanied by the substitution of Cu^{2+} with the Al^{3+} ions to be occurred in the HY framework to form the Si–O–Cu bond. The particle size of the CuO could be also controlled by the current density, which results in better dispersion of the CuO nanoparticles on the HY surface.

3.2.2. Kinetic study

The kinetics of the photocatalytic activity rate of most organic compounds is described by pseudo first order kinetics:

$$Ln\left(\frac{C_o}{C_t}\right) = k't \quad (20)$$

where k' is the rate constant, t is the reaction time, and C_o and C_t are the initial concentration and concentration at time t of MG, respectively. Fig. 9 shows that the photocatalytic activity of CuO/HY prepared at current densities of 10, 30, and 120 mA cm^{-2} for the decolorization of MG follows the pseudo first order kinetic perfectly. The k' values are calculated to be 0.0038, 0.0027 and 0.0018 min^{-1}, which means that they decrease with increasing current density. These results provide further verification supporting the efficient performance of the CuO/HY prepared at 10 mA cm^{-2}.

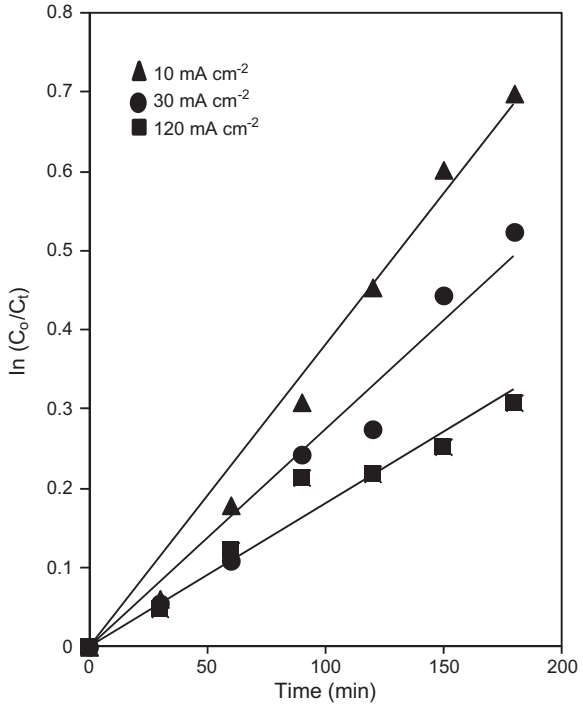

Fig. 9. Pseudo first order kinetic model for photodecolorization of MG (pH 4, 0.38 g L^{-1}, 15 mg L^{-1} initial MG concentration).

3.2.3. Determination of apparent activation energy

A series of experiments was performed at varying reaction temperatures from 303 to 323 K in order to determine the effect of the apparent activation energy (E_a) on the photocatalytic decolorization of MG. E_a was calculated from the Arrhenius equation as follows [42]:

$$k_{app} = A\exp^{-Ea/RT} \quad (21)$$

where A is a temperature independent factor (1 h^{-1}), E_a is the apparent activation energy of the photocatalytic decolorization (J mol^{-1}), R is the gas constant (8.314 J K mol^{-1}), and T is the solution temperature.

As shown in Fig. 10, the plot of In (k_{app}) versus $1/T$ gives a linear relationship. The slope of this straight line is equal to $-E_a/R$, and thus the calculated apparent activation energies were 22.9, 37.5 and 75.8 kJ mol^{-1} for CuO/HY catalysts prepared under current densities of 10, 30, and 120 mA cm^{-2}, respectively. The result also supports the efficiency of photodecolorization of MG using CuO/HY catalyst prepared under lower current density.

3.2.4. Reusability

The reusability of photocatalyst was important to establish its stability for practical application [43]. In this study, only a slight decrease in the percentage decolorization, from 97% to 89%, was detected for at least six reaction cycles (Fig. 11). In all cases, after each cycle, the CuO/HY catalyst was simply recovered by filtration, dried overnight, and calcined at 550 °C for 3 h before being reused in a successive batch. This result indicated that the CuO/HY catalyst prepared under a current density of 10 mA cm^{-2} is a stable photocatalyst in which deactivation hardly occurred during the reaction.

3.2.5. Degradation of MG

Chemical oxygen demand (COD) and total organic carbon (TOC) analyses were carried out before and after 180 min of irradiation in order to study the toxicity and degradability of the 10 mg L^{-1} MG solution over CuO/HY catalyst prepared at 10 mA cm^{-2} (Fig. 12). The COD result showed a decrease in the concentration of MG from 68 to 9 mg L^{-1}, indicating that 87% degradation of MG molecules had occurred after 3 h of reaction. The TOC also decreased from 29 to 5 mg L^{-1}, demonstrating that only 18% of TOC remained in

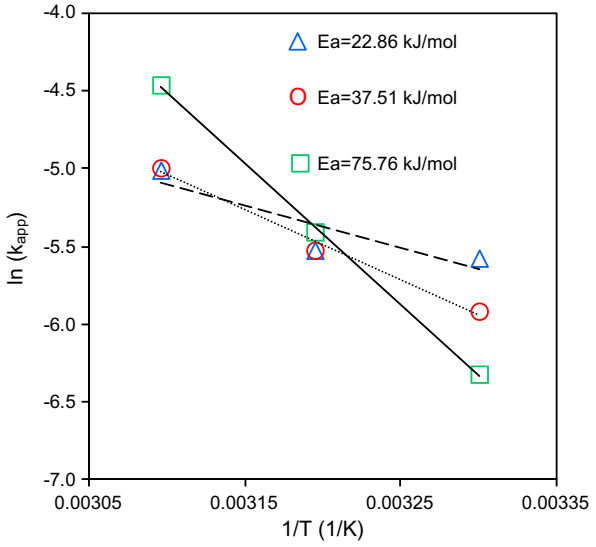

Fig. 10. Apparent activation energy for decolorization of MG using CuO/HY catalysts prepared under various current density. (△) 10 mA cm^{-2} (○) 40 mA cm^{-2} (□) 120 mA cm^{-2}. (pH 4, 0.38 g L^{-1}, 15 mg L^{-1} initial dye concentration).

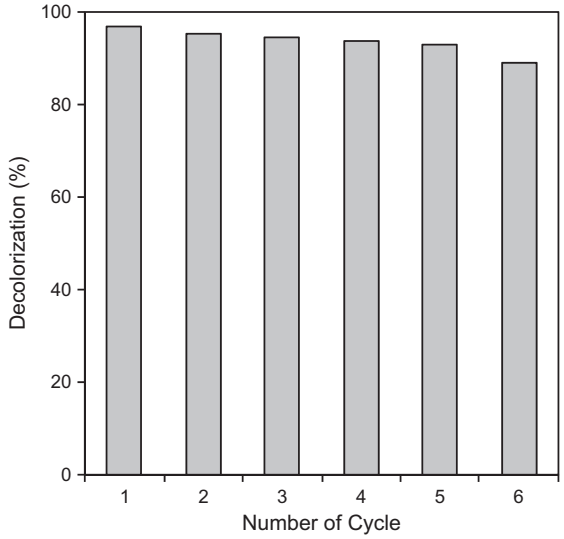

Fig. 11. Reusability of CuO/HY (10 mA cm^{-2}) on photocatalytic decolorization of MG (pH 4, 0.38 g L^{-1}, 10 mg L^{-1} initial MG concentration).

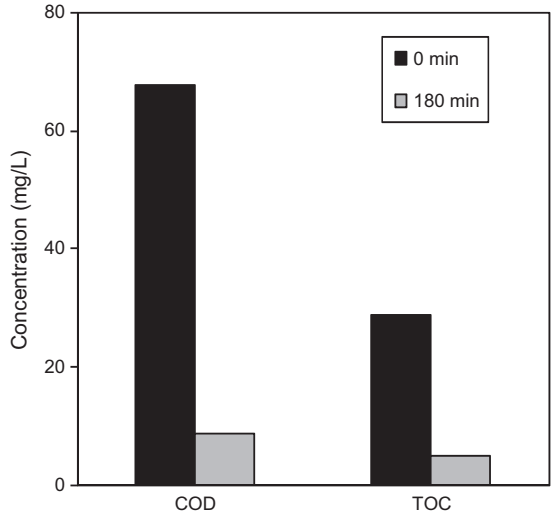

Fig. 12. The graph of COD removal and TOC reduction levels after 180 min of reaction.

the solution due to the formation of some long-lived byproducts which resist further degradation.

The degradation of MG molecules occurs when the hydroxyl radical attack to the central carbon atom of MG to form *N*,*N*-dimethylamino phenyl ring then was converted into two different compounds known as *N*,*N*-dimethyl-benzenamine and 4-dimethylamino-benzophenone [44]. The *N*,*N*-dimethyl-benzenamine was attacked by hydroxyl radicals to give a reactive cationic radical and demethylated to form benzenamine, and further oxidized to nitrobenzene. Next, the 4-dimethylamino-benzophenone is demethylated to form 4-amino-benzophenone and oxidized to 4-nitrobenzophenone before converted to benzophenone and NO_3^-. The cleavage of benzophenone yields benzaldehyde and benzene. The complete mineralization followed by ring opening of aromatic compounds contributed in the formation of CO_2 and H_2O.

4. Conclusion

CuO/HY catalysts have been successfully prepared by a simple electrolysis method under three different levels of current density: 10, 30, and 120 mA cm^{-2}. The surface area analysis indicated that the size of the CuO/HY particles decreased while the surface area and pore volume increased with increasing current density. These properties led to an increase in the band gap energy due to the quantum size effect. Cu nanoparticles were formed during the electrolysis and were then oxidized to CuO after drying/calcination and distributed well on the CuO/HY catalyst surface, as verified by XRD, FTIR, and UV–Vis analyses. In parallel, dealumination accompanied by isomorphous substitution of Cu^{2+} also occurred in the HY framework during the electrolysis, as confirmed by the FTIR and pyridine adsorption FTIR results. The formation of Si–O–Cu bonds was found to increase due to the decrease in the current density, which then enhanced the performance of the photoactive decolorization of MG. These findings show the possible controllable ion exchange capacity, acidity, particle size, and band gap energy of the photocatalyst. The CuO/HY catalysts prepared at a current density of 10 mA cm^{-2} demonstrated the highest photoactive performance compared to the others. The decrease of >83% in the COD and TOC analyses confirmed the degradability of the MG solution over the CuO/HY catalyst. The good stability found in the reusability studies is expected to widen the potential applications of CuO/HY. In addition, it is also believed that the electrosynthesis system studied could be applied for synthesis of various supported metal catalysts.

References

[1] A.A. Jalil, S. Triwahyono, S.H. Adam, N.D. Rahim, M.A.A. Aziz, N.H.H. Hairom, N.A.M. Razali, M.A.Z. Abidin, M.K.A. Mohamadiah, J. Hazard. Mater. 181 (2010) 755–762.
[2] Y.M. Slokar, A. Majcen Le Marechal, Dyes Pigments 37 (1998) 335–356.
[3] C. Galindo, P. Jacques, A. Kalt, Chemosphere 45 (2001) 997–1005.
[4] M. Iranifam, M. Zarei, A.R. Khataee, J. Electroanal. Chem. 659 (2011) 107–112.
[5] S. Garcia-Segura, A. El-Ghenymy, F. Centellas, R.M. Rodríguez, C. Arias, J.A. Garrido, P.L. Cabot, E. Brillas, J. Electroanal. Chem. 681 (2012) 36–43.
[6] A. Nezamzadeh-Ejhieh, Z. Salimi, Appl. Catal. A: Gen. 390 (2010) 110–118.
[7] A. Batista, H. Carvalho, G. Luz, P. Martins, M. Gonçalves, L. Oliveira, Environ. Chem. Lett. 8 (2010) 63–67.
[8] H.D. Liu, S.L. Zhou, Y. Wang, Y. Xu, Y. Cao, J.H. Zhu, in: M.C.E. van Steen, L.H. Callanan (Eds.), Stud. Surf. Sci. Catal., Elsevier, 2004, pp. 2527–2535.
[9] H.L. Xia, H.S. Zhuang, T. Zhang, D.C. Xiao, J. Environ. Sci. 19 (2007) 1141–1145.
[10] D.M. Fernandes, R. Silva, A.A.W. Hechenleitner, E. Radovanovic, M.A.C. Melo, E.A.G. Pineda, Mater. Chem. Phys. 115 (2009) 110–115.
[11] I. Lisiecki, J. Phys. Chem. B 109 (2005) 12231–12244.
[12] A. Nezamzadeh-Ejhieh, S. Hushmandrad, Appl. Catal. A: Gen. 388 (2010) 149–159.
[13] R.S. Bowman, Microporous Mesoporous Mater. 61 (2003) 43–56.
[14] A.A. Jalil, N. Kurono, M. Tokuda, Synlett 12 (2001) 1944–1946.
[15] A.A. Jalil, N. Kurono, M. Tokuda, Synthesis 18 (2002) 2681–2686.
[16] S. Triwahyono, A.A. Jalil, R.R. Mukti, M. Musthofa, N.A.M. Razali, M.A.A. Aziz, Appl. Catal. A: Gen. 407 (2011) 91–99.
[17] M.A.A. Aziz, N.H.N. Kamarudin, H.D. Setiabudi, H. Hamdan, A.A. Jalil, S. Triwahyono, J. Nat. Gas Chem. 21 (2012) 29–36.
[18] N.H.N. Kamarudin, A.A. Jalil, S. Triwahyono, R.R. Mukti, M.A.A. Aziz, H.D. Setiabudi, M.N.M. Muhid, H. Hamdan, Appl. Catal. A: Gen. 431–432 (2012) 104–112.
[19] N.F. Jaafar, A.A. Jalil, S. Triwahyono, M.N.M. Muhid, N. Sapawe, M.A.H. Satar, H. Asaari, Chem. Eng. J. 191 (2012) 112–122.
[20] N. Sapawe, A.A. Jalil, S. Triwahyono, S.H. Adam, N.F. Jaafar, M.A.H. Satar, Appl. Catal. B: Environ. 125 (2012) 311–323.
[21] N. Sapawe, A.A. Jalil, S. Triwahyono, Chem. Eng. J. (2013), http://dx.doi.org/10.1016/j.cej.2013.03.121.
[22] A.A. Jalil, N. Kurono, M. Tokuda, Tetrahedron 58 (2002) 7477–7484.
[23] N. Kurono, T. Inoue, M. Tokuda, Tetrahedron 61 (2005) 11125–11131.
[24] R.M. Mohamed, M.M. Mohamed, Appl. Catal. A: Gen. 340 (2008) 16–24.
[25] Y. Hu, L. Dong, M. Shen, D. Liu, J. Wang, W. Ding, Y. Chen, Appl. Catal. B: Environ. 31 (2001) 61–69.
[26] P. Wang, X. Zheng, X. Wu, X. Wei, L. Zhou, Microporous Mesoporous Mater. 149 (2012) 181–185.
[27] C.H. Xu, C.Q. Liu, Y. Zhong, X.Z. Yang, J.Y. Liu, Y.C. Yang, Z.X. Ye, Chin. Chem. Lett. 19 (2008) 1387–1390.
[28] M. Srivastava, A.K. Ojha, S. Chaubey, P.K. Sharma, A.C. Pandey, J. Alloys Compd. 494 (2010) 275–284.
[29] M.R. Nunes, O.C. Monteiro, A.L. Castro, D.A. Vasconcelos, A.J. Silvestre, Eur. J. Inorg. Chem. (2008) 961–965.
[30] S.F. Wang, H. Yang, T. Xian, X.Q. Liu, Catal. Commun. 12 (2011) 625–628.
[31] S.N. Sahu, K.K. Nanda, PINSA 67A (2001) 103–130.
[32] J. Scherzer, J.L. Bass, J. Catal. 28 (1973) 101–115.

[33] R. Cid, F.J.G. Llambías, J.L.G. Fierro, A.L. Agudo, J. Vlllaseñor, J. Catal. 89 (1984) 478–488.
[34] J.R. Ferraro, Low-frequency Vibrations of Inorganic and Coordination Compounds, Plenum Press, NY, 1971.
[35] C.M. Parler, J.A. Ritter, M.D. Amiridis, J. Non-Cryst. Solids 279 (2001) 119–125.
[36] N. Sapawe, A.A. Jalil, S. Triwahyono, R.N.R.A. Sah, N.W.C. Jusoh, N.H.H. Hairom, J. Efendi, Appl. Catal. A: Gen. 456 (2013) 144–158.
[37] H.D. Setiabudi, A.A. Jalil, S. Triwahyono, N.H.N. Kamarudin, R.R. Mukti, Appl. Catal. A 417–418 (2012) 190–199.
[38] S. Krijnen, Titanium Epoxidation Catalysts: Zeolite and Silsesquioxane Based Materials, Eindhoven University of Technology, Netherlands, 1998.
[39] Y. Kuwahara, J. Aoyama, K. Miyakubo, T. Eguchi, T. Kamegawa, K. Mori, H. Yamashita, J. Catal. 285 (2012) 223–234.
[40] J. Grzechulska, A.W. Morawski, Appl. Catal. B: Environ. 36 (2002) 45–51.
[41] W. Liu, L. Cao, G. Su, H. Liu, X. Wang, L. Zhang, Ultrason. Sonochem. 17 (2010) 669–674.
[42] A.A. Jalil, S. Triwahyono, M.R. Yaakob, Z.Z.A. Azmi, N. Sapawe, N.H.N. Kamarudin, H.D. Setiabudi, N.F. Jaafar, S.M. Sidik, S.H. Adam, B.H. Hameed, Bioresour. Technol. 120 (2012) 218–224.
[43] J. Li, F. Sun, K. Gu, T. Wu, W. Zhai, W. Li, S. Huang, Appl. Catal. A: Gen. 406 (2011) 51–58.
[44] C. Berberidou, I. Poulios, N.P. Xekoukoulotakis, D. Mantzavinos, Appl. Catal. B: Environ. 74 (2007) 63–72.